Molecular Dynamics Study of Anisotropic Translational and Rotational Diffusion in Liquid Benzene

M. Schwartz,*,† D. Duan,‡ and R. J. Berry*,‡

Department of Chemistry, University of North Texas, Denton, Texas 76203-507, and Air Force Research Laboratory Materials and Manufacturing Directorate, Wright-Patterson AFB, Ohio 45433

Received: June 8, 2005; In Final Form: July 16, 2005

Equilibrium NPT and *NVT* molecular dynamics simulations were performed on liquid benzene over an extended range of temperature (from 260 to 360 K) using the COMPASS force field. Densities and enthalpies of vaporization (from cohesive energy densities) were within 1% of experiment at all temperatures. tumbling and spinning rotational diffusion coefficients, $D_\perp$ and $D_{||}$, computed as a function of temperature, agreed qualitatively with the results of earlier reported experimental and computational investigations. Generally, it was found that $D_{||}/D_\perp \approx 1.4-2.5$ and the activation energy for tumbling was significantly greater than for spinning about the C_6 axis [$E_a(D_\perp) = 8.1$ kJ mol^{-1} and $E_a(D_{||}) = 4.5$ kJ mol^{-1}]. Calculated translational diffusion coefficients were found to be in quantitative agreement with experimental values at all temperatures [deviations were less than the scatter between different reported measurements]. In addition, translational diffusion coefficients were computed in the molecule-fixed frame to yield values for D_{xy} (diffusion in the plane of the molecule) and D_z (diffusion perpendicular to the plane). It was found that the ratio $D_{xy}/D_z \approx 2.0$, and that the two coefficients have roughly equal activation energies. This represents the first atomistic molecular dynamics study of translational diffusion in the molecular frame.

Introduction

In the past ∼30 years, there have been numerous experimental investigations on the reorientational dynamics in liquid benzene, using NMR relaxation, vibrational line shapes and depolarized Rayleigh line widths. The great majority of these studies show that rotational diffusion in this oblate symmetric top is highly anisotropic, with parallel, "spinning", diffusion coefficients ($D_{||}$) significantly higher than the perpendicular, "tumbling", coefficients ($D_\perp$). The rotational anisotropy in liquid benzene has also been verified by a number of Molecular Dynamics simulations.

One expects intuitively that, like molecular reorientation, translational diffusion in benzene should also be anisotropic, with differing diffusion coefficients for motion parallel and perpendicular to the symmetry axis. Unfortunately, in contrast to rotational motion, there are no experimental methods by which one can monitor translational diffusion components along various molecular axes in isotropic fluids. However, as will be shown below, it is possible to analyze MD simulation data to extract molecule-fixed diffusion coefficients in symmetric-top molecules such as benzene.

The goal of this work is to utilize molecular dynamics simulations to investigate the anisotropy of both translational and reorientational diffusion in benzene as a function of temperature throughout the liquid range. The computational methods and the results are presented and discussed below.

Computational Methods

The COMPASS [1−4] force field was used for all minimization and molecular dynamics runs. The valence terms in this force field are similar to those in earlier class II force fields (e.g., references in ref 3), and include stretching, bending and torsional terms + cross-terms involving two or three coordinates. It also includes an out-of-plane potential term to preserve planarity in aromatic systems. The principal difference from earlier force fields is that the COMPASS nonbond parameters (van der Waals and electrostatic) were developed to match experimental densities and enthalpies of vaporization (derived from computed cohesive energy densities) of suitable reference compounds at individual state points. The aromatic carbon nonbond parameters were determined by matching calculated values of these quantities with experiment for benzene (at 298 K) as well as for several substituted benzenes at individual temperatures.

Cubic cells containing 108 benzene molecules were built via a Monte Carlo algorithm as implemented in the *Accelrys*[5] Amorphous Cell module. Cells were then equilibrated at temperatures from 260 K (super cooled liquid) to 360 K (superheated liquid) using NPT dynamics (with an Andersen thermostat[6] and Berendsen barostat[7]) for a period of 2 ns (with 1 fs time steps). Equilibrated cell volumes ranged from ∼25−26 Å^3, and were used to calculate densities at each temperature.

The cells were further equilibrated at each temperature using *NVT* dynamics (Berendsen thermostat) for a period of 200 ps, followed by production runs for (a) 200 ps (with snapshots every 0.1 ps) and (b) 20 ps (with snapshots every 0.002 ps). These latter runs were used to compute reorientational/translational diffusion coefficients, as well as cohesive energy densities (and derived enthalpies of vaporization). A nonbonded group-based cutoff of 10 Å was used for all runs.

Although not shown in the interest of brevity, computed densities and enthalpies of vaporization of benzene were within 1% and 1.5%, respectively, of experimental values at all temperatures over the 100 K range.

† University of North Texas.
‡ Wright-Patterson AFB.

10.1021/jp0530799 CCC: $30.25
Published on Web 08/26/2005

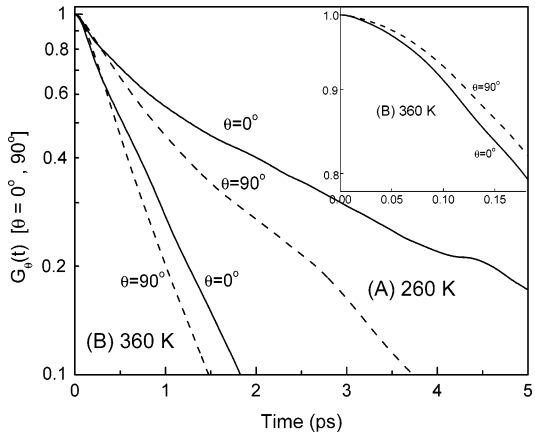

Figure 1. Correlation functions, $G_\theta(t)$: solid line, $\theta = 0°$; dashed line, $\theta = 90°$; (A) $T = 260$ K; (B) $T = 360$ K. Inset: short-time correlation functions at $T = 260$ K.

Results and Discussion

A. Rotational Diffusion. Because benzene is an oblate symmetric-top, its reorientation in the liquid can be characterized by two independent rotational diffusion coefficients, $D_\perp$ and $D_{||}$, which represent the rates of "tumbling" of the principal axis and "spinning" about this axis, respectively. To calculate the values of these quantities, one must first determine the rotational correlation functions of two separate unit vectors (**u**) in the molecule, oriented at different angles (θ) with respect to the symmetry axis. These correlation functions are given by

$$G_\theta(t) = \langle P_2[\cos\{\alpha(t)\}]\rangle = \left\langle \frac{1}{2}[3\cos^2\{\alpha(t)\} - 1]\right\rangle \quad (1)$$

P_2 is the second-order Legendre polynomial, $\cos\{\alpha(t)\}$ is the cosine of the angle by which the vector has rotated in the time, t; it is obtained from the relation $\cos\{\alpha(t)\} = \mathbf{u}(0)\cdot\mathbf{u}(t)$, which is the scalar product of the unit vector at zero time and a later time. The angular brakets indicate an ensemble average. Two separate unit vectors were monitored, one in the plane of the benzene molecule ($\theta = 90°$ relative to the symmetry axis) and the second vector along the axis ($\theta = 0°$), i.e., normal to the plane (constructed from the cross-product of two orthogonal in-plane vectors). To compute the correlation functions, we have averaged over all molecules in the liquid and over multiple time origins.[8]

Displayed in Figure 1 are representative rotational correlation functions at the two temperature extremes (the inset shows the short-time behavior of the functions at the higher temperature). One observes from the figure that the correlation function, $G_0(t)$ (solid curves), decays more slowly than does $G_{90}(t)$ (dashed curves) at intermediate to long times, indicating that the vector normal to the plane is rotating more slowly than the in-plane unit vector. Further, as expected, both correlation functions decay more rapidly at higher temperature, as a result of the enhanced rate of rotation. Although there is more noise in the functions at lower temperature (due to the averaging of fewer time origins at greater values of t), one finds that the functions become essentially exponential (linear on a semilogarithmic scale) at longer times, indicating that the rotation is diffusional in nature (i.e., the result of numerous collisions in the liquid). On the other hand, at very short times, the decay is markedly nonexponential (figure inset), denoting the "free rotation" regime, where the reorientation is essentially that of a free rotor. It is of interest to note that the relative short-time decay rates of the two vectors is opposite that at longer times. On reflection, it is not surprising that $G_0(t) < G_{90}(t)$ at short times, where the rotation is inertially controlled. This is because rotation of the normal vector ($\theta = 0°$) is dependent only upon the moment of inertia component in the plane of the molecule, $I_\perp$, which is smaller (by a factor of 2) than the inertia component about the symmetry axis ($I_{||}$). Rotation of the in-plane vector ($\theta = 90°$) is dependent upon both $I_\perp$ and $I_{||}$ and is therefore slower at short times.

TABLE 1: Reorientational Correlation Times and Diffusion Coefficients

T (K)	$\tau(00)$ (ps)	$\tau(900)$ (ps)	$10^{-9}D_\perp$ (s^{-1})	$10^{-9}D_{||}$ (s^{-1})	ρ^a
260	2.25	1.42	74	182	2.5
270	1.59	1.20	105	181	1.7
280	1.69	1.11	99	223	2.3
290	1.63	1.17	102	195	1.9
300	1.16	0.90	144	236	1.6
310	1.15	0.93	145	219	1.5
320	1.00	0.81	167	252	1.5
330	0.99	0.77	168	275	1.6
340	0.87	0.73	192	270	1.4
350	0.76	0.61	219	338	1.5
360	0.78	0.65	214	306	1.4
$E_a{}^b$			8.1	4.5	
SD(E_a)^b			0.6	0.6	

^{a} $D_\perp/D_{||}$. ^{b} Activation energy in kJ mol^{-1}.

The rotational correlation time, $\tau(\theta)$, is most commonly taken as the area under the correlation function (which is consistent with the value obtained experimentally from NMR relaxation time measurements). To minimize the effect of noise in the wings (primarily at low temperature), it was assumed that the correlation functions were exponential at long times (for $G_\theta \leq 0.3$) when numerically computing the areas.

Shown in Table 1 are the rotational correlation times for the in-plane [$\tau(90°)$] and normal [$\tau(0°)$] unit vectors as a function of temperature. Consistent with the relative rates of decay of $G_0(t)$ and $G_{90}(t)$ (Figure 1), one finds that $\tau(90°) < \tau(0°)$ at all temperatures. These two values of the correlation times can be used to determine the "tumbling" and "spinning" reorientational diffusion constants, $D_\perp$ and $D_{||}$, from an equation first derived by Woessner:[9]

$$\tau(\theta) = \int_0^\infty P_2(\cos\theta(t))\,dt = \frac{\frac{1}{4}(3\cos^2\theta - 1)^2}{6D_\perp} + \frac{3\sin^2\theta\cos^2\theta}{5D_\perp + D_{||}} + \frac{\frac{3}{4}\sin^4\theta}{2D_\perp + 4D_{||}} \quad (2)$$

Note that for $\theta = 0°$, eq 2 reduces to $\tau(0°) = (6D_\perp)^{-1}$. One can then use $D_\perp$ and $\tau(90°)$ directly in this equation to calculate $D_{||}$. The numerical values of both rotational diffusion coefficients are given in Table 1, and an Arrhenius temperature plot of the two diffusion constants is displayed in Figure 2. One observes that $D_{||}$ (squares) is significantly greater than $D_\perp$ (circles) at all temperatures, with a rotational anisotropy, $\rho = D_{||}/D_\perp$, ranging from ~2.5 at the lowest temperatures to ~1.5 in the superheated liquid (Table 1). The computed activation energies for the two rotational motions are $E_a(D_\perp) = 8.1 \pm 0.6$ (1 SD) kJ mol^{-1} and $E_a(D_{||}) = 4.5 \pm 0.6$ (1 SD) kJ mol-^{1}. These observations [$D_{||} > D_\perp$ and $E_a(D_\perp) > E_a(D_{||})$] are qualitatively similar to results reported in other experimental studies[10−22] and MD simulations[10,23−26] of liquid benzene.

Experimentally, one most commonly utilizes the reorientational contribution to Raman bandwidths of A_{1g} vibrational

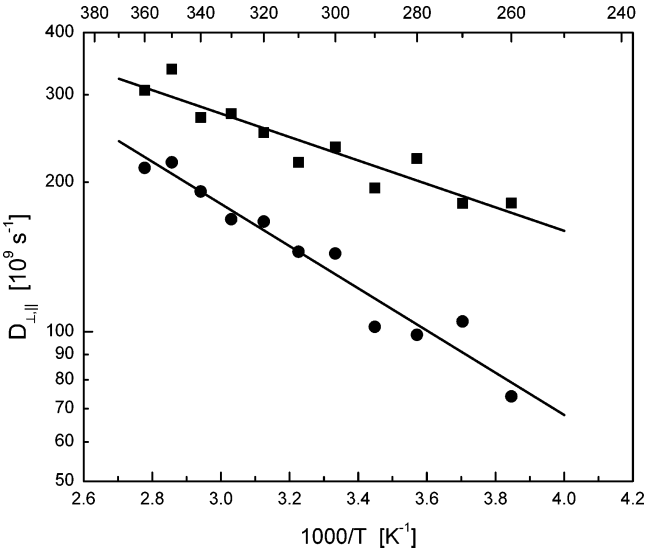

Figure 2. Rotational diffusion coefficients: circles, $D_\perp$; squares, $D_\parallel$. The lines represent the best least-squares fit to the computed data.

modes, or Rayleigh scattering line widths to determine $\tau_2(0°)$.[27] Raman line widths of degenerate modes can also be used to compute $\tau_2(90°)$. NMR relaxation time measurements [either $^1H-^{13}C$ dipole−dipole or ^2D quadrupole in C_6D_6] can be utilized to obtain $\tau_2(90°)$. $\tau_2(0°)$ can also be determined from DD/CSA cross-relaxation experiments.

To afford a semiquantitative comparison of our rotational diffusion coefficients with earlier studies, we have tabulated many of the earlier reported results (both experiment and MD) in Table 2; other tabulations are reported in ref 26 (correlation times) and ref 10 (diffusion coefficients). In studies where only correlation times are reported, we have converted them to diffusion constants, using eq 2 above. In most cases, the ambient temperature reported was somewhat different from 298 K. These data were converted to 298 K using our computed activation energies (vide supra).

It may be seen from the data in Table 2A (298 K diffusion constants) that, as discussed by Dölle and co-workers[10] in a recent comprehensive joint NMR/MD investigation, there is a broad range of reported diffusion coefficients, even from recent investigations, most likely arising, at least in part, from the different methods used to determine them experimentally and the differing force fields used in the MD studies. At most, it can be said that our room temperature (interpolated) tumbling diffusion constant (128×10^9 s^{-1}) is somewhat above the range reported in earlier studies ($\sim(90-100) \times 10^9$ s^{-1}), and that our spinning diffusion coefficient (227×10^9 s^{-1}) falls within the general range ($\sim(140-290) \times 10^9$ s^{-1}). The reorientational anisotropy, $\rho = 1.8$, is also within the range of other reported values. From Table 2B, it is seen that there is a similarly broad variation in activation energies computed for $D_\perp$. Our value lies at the lower end, but in the range of earlier reported results. We are aware of only one experimental determination of $E_a(D_\parallel)$;[10] as seen in the table, our computed activation energy is in satisfactory agreement with the value determined experimentally. The very low activation energy for spinning about the principal axis is consistent with "slip"[28] rather than "stick"[29] hydrodynamic boundary conditions,[11] because $E_a[D_\parallel]_{slip} = E_a[(T)^{1/2}] = 1.3$ kJ mol^{-1} vs $E_a[D_\parallel]_{stick} = E_a[T/\eta] = 13.8$ kJ mol^{-1}.

Because of the relatively broad range of experimental reorientational diffusion coefficients and their associated activation energies, no assessment of the COMPASS force field can be afforded by comparison of the simulated results with values from experiment.

TABLE 2: Comparison with Earlier Reported Reorientational Diffusion Coefficients

(A) Room Temperature (298 K) Diffusion Coefficients

method	year	ref	$10^{-9}D_\perp$ (s^{-1})	$10^{-9}D_\parallel$ (s^{-1})	$\rho_{rot.}$[a]
MD		this work	128	227	1.8
Raman	1972	11	66	52	0.8
Raman/NMR	1972	12	54	273	5.1
Raman/NMR	1978	13	76	180	2.4
IR/Raman	1979	14	89	180	2.0
Raman	1980	15	91	220	2.4
MD	1982	23	81	237	2.9
MD	1985	24	121	249	2.1
MD	1988	25	96	199	2.1
NMR	1991	16	108	169	1.6
NMR	1994	17	90	201	2.2
Raman	1996	22	90	253	2.8
NMR	1997	18	103	286	2.8
Raman/NMR	1998	26	78	217	2.8
MD	1998	26	95	143	1.5
NMR(DD + CSA)	2000	10	94	191	2.0
MD	2000	10	108	168	1.6

(B) Activation Energies

method	year	ref	$E_a(D_\perp)$ (kJ mol^{-1})	$E_a(D_\parallel)$ (kJ mol^{-1})
MD		this work	8.1	4.5
Rayleigh (C_6H_6)	1982		19	8.3
Rayleigh (C_6D_6)	1982		19	8.7
Rayleigh	1975	20	10.9	
Raman	1972	12	11.3	
NMR	1991	16	9.8	
NMR	2000	10	13.3	3.4
MD	2000	10	9.3	
Raman (diff ^2D isotopes)	1985	21	7.1−9.2	

[a] $D_\perp/D_\parallel$.

TABLE 3: Translational Diffusion Coefficients

T (K)	10^9D_{tr}(LF) (m^2 s^{-1})	10^9D_{tr}(MF) (m^2 s^{-1})	10^9D_z(MF) (m^2 s^{-1})	10^9D_{xy}(MF) (m^2 s^{-1})	ρ_{tr}[a]
260	0.98	1.48	0.98	1.73	1.8
270	1.32	2.17	1.36	2.58	1.9
280	1.84	2.33	1.28	2.86	2.2
290	1.85	2.47	1.47	2.97	2.0
300	2.82	3.55	2.41	4.12	1.7
310	2.45	3.10	1.80	3.76	2.1
320	3.04	3.81	2.70	4.37	1.6
330	4.03	4.71	3.03	5.55	1.8
340	3.78	4.56	2.68	5.50	2.1
350	4.69	5.15	2.93	6.26	2.1
360	4.86	5.34	3.22	6.40	2.0
E_a[b]	12.1	9.5	9.2	9.6	
SD(E_a)[b]	0.8	0.7	1.1	0.7	

[a] D_{xy}(MF)/D_z(MF). [b] Activation energy in kJ mol^{-1}.

B. Translational Diffusion. It is straightforward to compute the translational diffusion coefficient, D_{tr}, of a fluid from the long−time mean squared displacements, $\langle r^2 \rangle$, of the molecules' centers of mass (CM), as given by[8]

$$\langle r^2(t) \rangle = 6D_{tr}t \tag{3}$$

We have computed the diffusion coefficients in liquid benzene from the slopes $\langle r^2 \rangle$ vs t plots (in a linear region, ≥10 ps) as a function of temperature; the results are contained in the second column of Table 3 [D_{tr}(LF)]; the "LF" indicates that the displacements were computed in the system's laboratory frame.

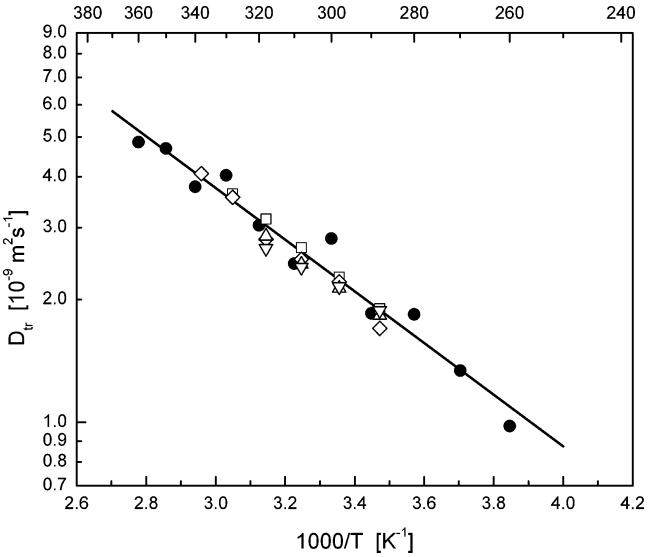

Figure 3. Experimental and calculated translational diffusion coefficients: filled circles (+line); this work (calculated); open triangles (down), ref 30; open triangles (up), ref 31; open diamonds, ref 32; open squares, ref 33.

An Arrhenius plot of the computed translational diffusion coefficients is presented in Figure 3, together with data from the earlier reported experimental determinations of D_{tr}.[30−33] As may be observed clearly from the figure, there is excellent *quantitative* agreement between theory and experiment. In addition, the activation energy of diffusion constants obtained from the MD simulations, $E_a(D_{tr}) = 12.1$ kJ mol^{-1} (Table 3), falls in the middle of the range of E_a's computed from the experimental data (8.9,[30] 11.2,[31] 12.8,[33] 13.7[32] kJ mol^{-1}). Thus, although the COMPASS force field was not parametrized directly for fluid transport properties, it is seen to yield quantitatively accurate translational diffusion coefficients of benzene throughout its liquid range.

There have been several earlier reported MD studies of benzene in which the translational diffusion coefficient has been computed either at a single temperature or over a range.[10,24,25] Although there is not a quantitative accord between theory and experiment observed here using the newer force field, the earlier results are in acceptable qualitative agreement with measured diffusion constants.

As discussed above, one observes very different rotational diffusion rates about the various axes in a symmetric top molecule. Intuitively, one also expects that the component of the translational diffusion coefficient parallel to the principal (z) axis should differ from the transverse (x and y) components. However, unlike molecular reorientation, translational diffusion coefficients parallel and perpendicular to the principal axis cannot be measured experimentally in an isotropic medium.

On the other hand, it *is* possible to use MD simulation data to compute the individual components of the overall CM displacement along the x, y, and z axes of a coordinate system fixed in the molecular frame. We have performed this calculation by decomposing the total displacement after a given 0.1 ps time step into x, y, and z components in the *molecule-fixed* reference frame at the beginning of the step. Then, the components of the various displacements have been summed, and averaged over time origins to yield mean-squared displacements, MSD(x), MSD(y) and MSD(z) as a function of time. The molecular frame will, of course, rotate relative to the laboratory frame as the molecule reorients. However, by using components decomposed along the molecule-fixed axes, we are determining the effective MSDs one would obtain in the absence of molecular rotation.

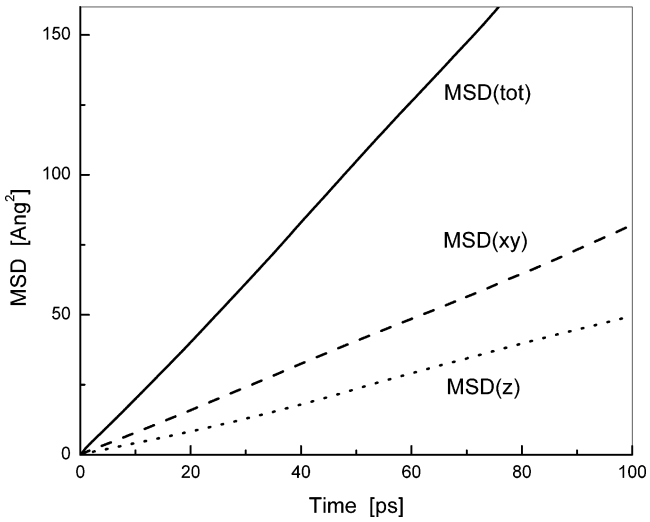

Figure 4. Mean squared displacements in the molecule-fixed frame at 300 K: solid line, total displacement [MSD(tot)]; dashed line, displacement in plane of molecule [MSD(xy): average of x and y components]; dotted line, displacement perpendicular to plane of molecule [MSD(z)].

The resulting plot for benzene (at 300 K) is displayed in Figure 4. In this figure, MSD(xy) represents the average of the x and y (transverse) squared displacements and MSD(tot) is the sum of all three squared components. It is observed clearly from the figure that the mean transverse displacement component, representing translation perpendicular to the principal axis increases much more rapidly with time than does the parallel displacement. One may compute a molecular frame overall diffusion coefficient, D_{tr}(MF) from eq 3 above. One can also calculate diffusion constants for motion perpendicular [D_{xy}(MF)] and parallel [D_z(MF)] from

$$\langle r_i^2(t)\rangle = 2D_{tr}(i)t \qquad (4)$$

where $\langle r_i^2(t)\rangle$ = MSD(xy) or MSD(z).

Values of D_{tr}(MF), D_z(MF), and D_{xy}(MF) were determined in this fashion and given in Table 3. It should be noted that these should be considered to be "effective" diffusion coefficients, representing what the rates of diffusion would be *if* the molecules were constrained from reorienting. Therefore, they cannot be compared directly with the diffusion coefficient in the laboratory frame. To the authors' knowledge, this represents the first application of an atomistic MD simulation to determine molecule-fixed translational diffusion constants in an isotropic liquid.

The overall molecular frame diffusion and the parallel and transverse components are plotted in Figure 5. One can see from both the table (ρ_{tr}) and figure that, as expected from the MSD plot (Figure 4), values of D_{xy}(MF) are greater than D_z(MF) at all temperatures, by approximately a constant factor of 2. This indicates that the in-plane translation of benzene through the fluid is around twice as rapid as motion parallel to the C_6 axis. One observes from the table that, unlike reorientational diffusion in benzene, for which $E_a(D_{||}) \ll E_a(D_\perp)$, activation energies for both molecular frame translational diffusion coefficients are relatively high and almost equal. This is not surprising because, in contrast to the spinning rotation, which requires no displacement of molecules in the first solvation sphere, both translations require significant rearrangement of neighboring molecules.

There have been no earlier reported determinations of the molecular frame components of benzene's translational diffusion constants. However, there have been two MD studies[24,26] in

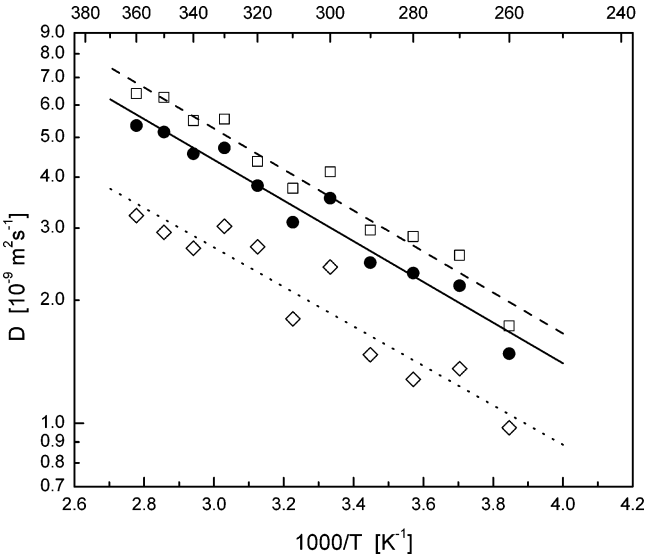

Figure 5. Translational diffusion coefficients in the molecule-fixed frame: filled circles (and solid line), D_{tr}(MF); open squares (and dashed line), D_{xy}(MF); open diamonds (and dotted line), D_z(MF).

which the velocity autocorrelation functions have been computed parallel and perpendicular to the molecular symmetry axis. In both cases, it was observed that the transverse velocity correlation times were significantly longer than the parallel (to the principal axis) times, by factors of ~1.5−2.0; these observations are consistent with our finding that $\rho_{tr} = D_{xy}(\mathrm{MF})/D_z(\mathrm{MF}) \approx 2$.

The Navier−Stokes hydrodynamic equations for components of the translational diffusion tensor in ellipsoidal molecules have been solved for 'stick' boundary conditions,[29] yielding analytical expressions for D_z(MF) and D_{xy}(MF) in terms of the major and minor semi-axis lengths (a and b), and the aspect ratio, κ.[34] Using benzene's molecular geometry[35] and C/H van der Waals radii,[36] it can be estimated that for benzene, $\kappa = 1.70$ Å/3.69 Å $= 0.46$. With the equations for the "stick" diffusion coefficients,[29] one predicts that the ratio of transverse to parallel (to the principal axis) diffusion coefficients should be $\rho = D_{xy}(\mathrm{MF})/D_z(\mathrm{MF}) \approx 1.4$, which is significantly below the observed ratio of ~2.0.

To the authors' knowledge, the only treatment of translational diffusion of ellipsoids with "slip" boundary conditions has been for prolate symmetric-tops,[37] for which it is predicted that $\rho_{tr} = D_{xy}(\mathrm{MF})/D_z(\mathrm{MF}) \approx \kappa^{-1}$, a result which is very different from the stick BC prediction. However, there have been recent nonatomistic MD simulations of molecular frame translation of both prolate and oblate ellipsoids.[38−40] In these cases, it has been observed from the simulations that for the prolates,[38,39] $\rho_{tr} \approx \kappa^{-1}$, in very good agreement with the analytical slip prediction, and that the same dependence of the translational anisotropy on κ^{-1} was observed for the oblate ellipsoids,[40] from which it may be inferred that the translational diffusion of both types of symmetric-tops is best characterized by the slip boundary condition. The results of our atomistic simulation of benzene here are also in agreement with this trend, in that $\rho_{tr}(2) \approx \kappa^{-1}(2.2)$.

Summary

The rotational diffusion of liquid benzene highly anisotropic at all temperatures, and numerical values of $D_\perp$ and $D_\parallel$ were found to be in qualitative agreement with the results of earlier simulations and experimental investigations. In the first atomistic simulation of translational diffusion coefficients in a molecule-fixed frame, it was observed that there is a similar anisotropy, with the transverse diffusion [D_{xy}(MF)] approximately twice as rapid as the parallel motion [D_z(MF)]. This result is in qualitative agreement with the prediction of the translation of ellipsoidal molecules using slip boundary conditions.

Acknowledgment. We acknowledge the WPAFB Materials Directorate, and the ASC and ARL Major Shared Resource Centers, operated by the DoD High Performance Computing and Modernization Office. M.S. thanks the Robert A. Welch Foundation [Grant B-657], the National Research Council [Air Force Summer Faculty Fellowship Program] and the Universal Technology Corporation for financial support.

References and Notes

(1) Sun, H.; Rigby, D. *Spectrochim. Acta, Part A* **1997**, *53*, 1301.
(2) Rigby, D.; Sun, H.; Eichinger, B. E. *Polym. Int.* **1997**, *44*, 311.
(3) Sun, H. *J. Phys. Chem. B* **1998**, *102*, 7338.
(4) Rigby, D. *Fluid Phase Equilib.* **2004**, *217*, 77.
(5) Accelrys Inc., 9685 Scranton Rd., San Diego, CA 92121-3752.
(6) Andersen, H. C. *J. Chem. Phys.* **1980**, *72*, 2384.
(7) Berendsen, H. J. C.; Postma, P. M.; van Gunsteren, W. F.; DiNola, A.; Haak, J. R. *J. Chem. Phys.* **1984**, *81*, 3684.
(8) Haile, J. M. *Molecular Dynamics Simulation: Elementary Methods*; John Wiley & Sons: New York, 1992.
(9) Huntress, W. T. *Adv. Magn. Reson.* **1970**, *4*, 1.
(10) Witt, R.; Sturz, L.; Dölle, A.; Müller-Plathe, F. *J. Phys. Chem. A* **2000**, *104*, 5716.
(11) Bartoli, F. J.; Litovitz, T. A. *J. Chem. Phys.* **1972**, *56*, 404.
(12) Gillen, K. T.; Griffiths, J. E. *Chem. Phys. Lett.* **1972**, *17*, 359.
(13) Tanabe, K. *Chem. Phys.* **1978**, *31*, 319.
(14) Tanabe, K. *Chem. Phys. Lett.* **1979**, *63*, 43.
(15) Tanabe, K.; Hiraishi, J. *Mol. Phys.* **1980**, *39*, 493.
(16) Dölle, A.; Suhm, M. A.; Weingärtner, H. *J. Chem. Phys.* **1991**, *94*, 3361.
(17) Coupry, C.; Chenon, M.-T.; Werbelow, L. G. *J. Chem. Phys.* **1994**, *101*, 899.
(18) Python, H.; Mutzenhardt, P.; Canet, D. *J. Phys. Chem. A* **1997**, *101*, 1793.
(19) Danninger, W.; Zundel, G. *Chem. Phys. Lett.* **1982**, *90*, 69.
(20) Patterson, G. D.; Griffiths, J. E. *J. Chem. Phys.* **1975**, *63*, 2406.
(21) Oehme, K.-L.; Seifert, F.; Rudakoff, G.; Carius, W.; Hölzer, W.; Schröter, O. *Chem. Phys.* **1985**, *92*, 169.
(22) Yi, J.; Jonas, J. *J. Phys. Chem.* **1996**, *100*, 16789.
(23) Steinhauser, O. *Chem. Phys.* **1982**, *73*, 155.
(24) Linse, P.; Engstrom, S.; Jonsson, B. *Chem. Phys. Lett.* **1985**, *115*, 95.
(25) Maliniak, A.; Laaksonen, A.; Kowalewski, J.; Stilbs, P. *J. Chem. Phys.* **1988**, *89*, 6434.
(26) Laaksonen, A.; Stilbs, P.; Wasylishen, R. E. *J. Chem. Phys.* **1998**, *108*, 455.
(27) Strictly speaking, Rayleigh scattering is coherent (unlike Raman) and, hence, reflects collected motions in the fluid. However, it is often assumed that the correlation time determined from Rayleigh line widths is approximately equal to the single particle correlation time.
(28) Hu, C.-M.; Zwanzig, R. *J. Chem. Phys.* **1974**, *60*, 4354.
(29) Shimizu, H. *J. Chem. Phys.* **1962**, *37*, 765.
(30) Graupner, K.; Winter, E. R. S. *J. Chem. Soc.* **1952**.
(31) Hiraoka, H.; Osugi, J.; Jono, W. *Rev. Phys. Chem. Jpn.* **1958**, *28*, 52.
(32) Rathbun, R. E.; Babb, A. L. *J. Phys. Chem.* **1961**, *65*, 5.
(33) Falcone, D. R.; Douglass, D. C.; McCall, D. W. *J. Phys. Chem.* **1967**, *71*, 2754.
(34) For an ellipse with semi-axes $a \times a \times b$, the aspect ratio is defined by $k = b/a$.
(35) Gauss, J.; Stanton, J. F. *J. Phys. Chem. A* **2000**, *104*, 2865.
(36) Bondi, A. *J. Phys. Chem.* **1964**, *68*, 441.
(37) Tang, S.; Evans, G. T. *Mol. Phys.* **1993**, *80*, 1443.
(38) Ravichandran, S.; Bagchi, B. *J. Chem. Phys.* **1999**, *111*, 7505.
(39) Vasanthi, R.; Ravichandran, S.; Bagchi, B. *J. Chem. Phys.* **2001**, *114*, 7989.
(40) Vasanthi, R.; Bhattacharyya, S.; Bagchi, B. *J. Chem. Phys.* **2002**, *116*, 1092.